

On a discontinuity at the base of the transition layer located between the Keplerian accretion disk and the compact object

L. Titarchuk¹ and I. Kalashnikov²

¹ Dipartimento di Fisica, Università di Ferrara, via Saragat 1, 44122 Ferrara, Italy
e-mail: titarchuk@fe.infn.it

² Keldysh Institute of Applied Mathematics, Russian Academy of Sciences. 4 Miusskaya sq., Moscow, 125047, Russia
e-mail: kalasxel@gmail.com

Received; accepted.

ABSTRACT

Context. We study the geometry of the transition layer (TL) between the classical Keplerian accretion disk (the TL outer boundary) and the compact object at the TL inner boundary.

Aims. Our goal is to demonstrate using the hydrodynamical formalism that the TL is created along with a shock due to a discontinuity and to an adjustment of the Keplerian disk motion to a central object.

Methods. We apply hydrodynamical equations to describe a plasma motion near a central object in the TL.

Results. We point out that before matter accretes to a central object the TL cloud is formed between an adjustment radius and the TL inner boundary which is probably a site where the emergent Compton spectrum comes from. Using a generalization of the Randkine-Hugoniot relation and a solution of the azimuthal force balance equation we have reproduced the geometric characteristics of TL.

Key words. accretion, accretion disks–radiation mechanisms: general– black hole physics–neutron stars–white dwarfs

1. Introduction

Accretion onto compact objects as white dwarf (WD), neutron star (NS), and black hole (BH) binaries are very similar. The accreting matter with relatively large angular momentum can form a disk or go to outflow (see Titarchuk et al. (2007) and Shaposhnikov & Titarchuk (2009), hereafter TSA07, ST09, respectively). On the other hand, the plasma with low angular momentum proceeds towards the compact object almost in a free-fall manner until the centrifugal force becomes strong to halt the flow (see, e.g., (Chakrabarti & Titarchuk 1995), hereafter CT95). Thus, we can suggest that three definitive regions (Keplerian disk, the shock, and a transition layer (TL) between the last stable orbit near WD, NS or BH and the shock, which are probably a place where the emergent X-ray spectrum is formed. In this paper, we study the characteristics of this adjustment of the Keplerian disk flow to an WD, an NS or an BH.

The disk starts to deviate from a Keplerian motion at a certain radius to adapt itself to the boundary conditions at WD or NS surface (or at the last stable orbit, at $r_1 = 3r_S$, where r_S is the Schwarzschild radius, in the case of a BH). Titarchuk et al. (1998) (hereafter TLM98) explained the millisecond variability detected by Rossi X-Ray Timing Explorer (RXTE) in the X-ray emission from a number of low-mass X-ray binary systems (XRBs). Later, Seifina & Titarchuk (2010), Farinelli & Titarchuk (2011), and so on analyzed X-ray data from Sco X-1, 4U 1728–34, 4U 1608–522, 4U 1636–536, 4U 0614–091, 4U 1735–44, 4U 1820–30, GX 5–1) in terms of dynamics of the centrifugal barrier, in a hot boundary region (the TL) surrounding a neutron star (NS). They demonstrated that this region may experience relaxation oscillations and that the displacements of a gas element both in radial and vertical direc-

tions occur at the same main frequency, of an order of the local Keplerian frequency.

Observations of black hole X-ray binaries and active galactic nuclei indicate that the accretion flows around black holes are composed of hot and cold gas, which have been theoretically described in terms of a hot corona next to an optically thick relatively cold disk. Liu & Qiao (2022) (hereafter LQ22) reviews the accretion flows around black holes, with an emphasis on the physics that determines the configuration of hot and cold accreting gas, and how the configuration varies with the accretion rate and thereby produces various luminosity and spectra. They provide references to the famous solutions of the standard disk model such as, for example, Shakura & Sunyaev (1973) (hereafter SS73). The most successful applications of this model are the steady state and time-dependent nature of thin disks in dwarf novae and soft X-ray transients. Application of the four accretion models to black holes presented by LQ22 is constrained by both the theoretical assumption of specific models and observational luminosity and spectrum.

The soft photons from the innermost part of the disk are scattered off the hot electrons thus forming the Comptonized X-ray spectrum [see Sunyaev & Titarchuk (1980), hereafter ST80]. The electron temperature is regulated by the supply of soft photons from a disk, which depends on the ratio of the energy release (accretion rate) in a disk and the energy release in the TL. For example, the electron temperature is higher for lower accretion rates (see, e.g., CT95), while for a high accretion rate (of an order of the Eddington one) the TL is cooled down very efficiently due to the soft photon flux and the Comptonization. This is a possible mechanism for the low-frequency QPOs (quasi-periodic oscillations), discovered by RXTE in a number of low-mass X-ray binary systems (LMXBs; see Strohmayer et al.

(1996); van der Klis et al. (1996), hereafter S96 and VK96a, respectively; Zhang et al. (1996), TLM98, Titarchuk et al. (2007) hereafter TSA07). These observations reveal a wealth of high and low-frequency X-ray variabilities that are believed to be due to the processes occurring in the very vicinity of an accreting NS and BH.

Lančová et al. (2019) discovered a new class of black hole accretion disk solutions through 3D radiative magnetohydrodynamic simulations applying the general relativity formalism. These solutions combine features of thin, slim, and thick disk models. They provide a realistic description of black hole disks and have a thermally stable, optically thick, Keplerian region supported by magnetic fields. Mishra et al. (2020) have conducted a detailed analysis of two-dimensional viscous, radiation hydrodynamic numerical simulations of the Shakura-Sunyaev thin disks around a stellar mass black hole. They found multiple robust, coherent oscillations occurring in the disk, including a trapped fundamental g-mode and standing-wave p-modes. The study suggests that these findings could be of astrophysical importance in observed twin peak, high-frequency QPOs. Large scale 3D magnetohydrodynamic simulations of accretion onto magnetized stars with tilted magnetic and rotational axes were done by Romanova et al. (2021). It was shown that the inner parts of the disc become warped, tilted, and precess due to magnetic interaction between the magnetosphere and the disc. According to results of the numerical simulations by Lugovskii & Chechetkin (2012), large-scale instability in accretion disks, reveals changes in a disk flow structure because of the formation of large vortices. Over time, this leads to the development of asymmetric spiral structures and results in angular-momentum redistribution within the disk.

Suková et al. (2017) have conducted simulations of accretion flows with a low angular momentum, filling the gap between spherically symmetric Bondi accretion and disc-like accretion flows. They identify ranges of parameters for which the shock after formation moves towards or outwards the central black hole or the long-lasting oscillating shock is observed. The results are scalable with a central black hole mass and can be compared to QPOs of selected microquasars and supermassive black holes in the centres of weakly active galaxies. In order to explain NICER telescope evidences for non-dipolar magnetic field structures in rotation-powered millisecond pulsars, Das et al. (2022) have conducted a suite of general relativistic magnetohydrodynamic simulations of accreting neutron stars for dipole, quadrupole, and quadrupolar stellar field geometries. The study found that the location and a size of the accretion columns resulting in hotspots changes significantly depending on initial stellar field strength and geometry, providing a viable mechanism to explain the radio power in observed neutron star jets.

Despite the increasing role of numerical simulations of accretion, the consideration of relatively simple analytical models allows us to identify the response of the system to changes in a set of parameters, which in the case of numerical simulations becomes a very cumbersome task. In the present paper we, along with other authors (e.g. Abramowicz & Fragile (2013); Ajay et al. (2022))), propose a model of accretion on the central object. The point is that existing models of shock waves (see e.g. Chakrabarti (1989)) cannot correctly describe the abrupt transition between the accretion disk and the TL. Our goal is to construct a satisfactory model of the shock wave lying at the base of TL, which can correctly describe observational data for temperature and density (Seifina & Titarchuk (2010)). In Sect. 2 we describe our approach to the TL model. In Sect. 3. we formulate equations to determine the vertical dependencies of density

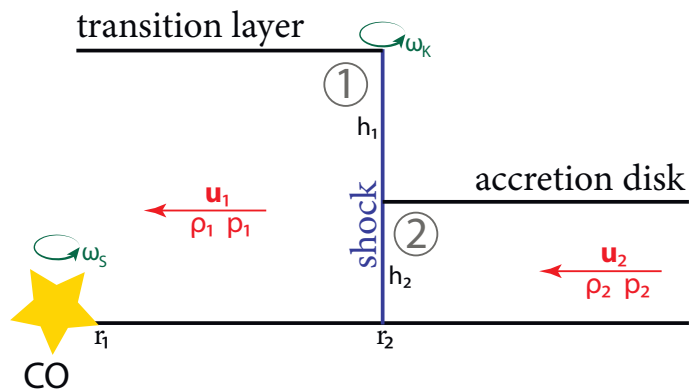


Fig. 1. The schematic representation of the considered model.

and pressure in the TL. In Secs. 4-5 we introduce the generalized Rankine-Hugoniot relation and take into account the rotation effect in the TL, respectively. We discuss our setup and final results in Sect. 6. Finally, we summarize our conclusions in Sect. 7.

2. Motivation and the model

Consideration of the two-dimensional structure of accretion disks is associated with obvious mathematical difficulties. Typically, a two-dimensional structure is only accounted for by a non-homogeneous distribution of matter within a layer of constant thickness $2h$. Consideration of a disk of constant thickness is made possible by ignoring the vertical velocity v_z . The more general case $h = h(r)$ requires solving equation $dh/dr = (v_z/u)|_{z=h(r)}$, where u is the radial velocity, to describe the behavior of the height as the radius changes.

According to the observations and their interpretations (TLM98, ST09) the disk height may achieve very significant values near the TL, while at larger distances it is pretty small. The thermodynamic characteristics of the plasma change considerably: in the TL, its temperature can reach tens of keV and its density drops drastically (see e.g. ST09). This change is widely believed to be presumably due to the presence of a shock wave (see e.g. CT95, TLM98 and ST09). Such a region near the central object (CO) is associated with the TL.

In an attempt to get closer to a two-dimensional consideration, we have chosen the following model describing the shock (Fig. 1). The flow velocity is supposed to have only radial and azimuthal components in the both sides of the shock, which are independent of the height. It is assumed that the height of the flow changes sharply by discontinuity from h_2 (the disk thickness) to h_1 (the TL thickness).

We require the angular velocity ω of the TL to match to the CO at its surface and coincide with disk velocity at the shock position r_2 . This angular velocity of the disk is supposed to equal to Keplerian one. Only $r\phi$ component of the viscous stress tensor was considered because it is responsible for taking off the angular momentum. We considered the stress tensor form $\eta r \omega'$, where η is the turbulent viscosity.

The thermodynamic quantities of the flow have vertical dependencies which are determined by the CO gravity and an equation of state. In order to identify them, we did not assume the smallness of the vertical coordinate compared to the radial one.

3. The vertical dependences

Let us start with the hydrostatic balance equation in the vertical direction:

$$\frac{\partial p}{\partial z} = -\rho \frac{\partial \Phi}{\partial z}, \quad (1)$$

where p , ρ are pressure and density and Φ is the gravitational potential created by the central object. We supposed that the vertical distribution of matter is given by polytropic relation $p = K\rho^{1+1/n}$, where K is a constant related to the entropy and n is the polytropic index. Then the formal solution of (1) may be written as:

$$K(n+1)\rho^{1/n} = \tilde{f}(r) - \Phi(r, z), \quad (2)$$

where \tilde{f} is an arbitrary function. We require the density and pressure to be zero at the inner boundary $z = \pm h$ and equal to some functions ρ_e , p_e correspondingly at the equator $z = 0$. Then we have:

$$\rho = \rho_e(r) \left(\frac{\Phi(r, h) - \Phi(r, z)}{\Phi(r, h) - \Phi(r, 0)} \right)^n, \quad (3)$$

$$p = p_e(r) \left(\frac{\Phi(r, h) - \Phi(r, z)}{\Phi(r, h) - \Phi(r, 0)} \right)^{n+1}. \quad (4)$$

Assuming the height is small compared to the radius $|z| \ll r$ we may get the usually used (Hōshi (1977); Matsumoto et al. (1984)) dependence $\rho = \rho_e(r)(1 - z^2/h^2)^n$. However, we did not make such an assumption later on.

We will need integrals from such vertical dependencies:

$$\zeta_n(r, h) = \int_{-h}^h \left(\frac{\Phi(r, h) - \Phi(r, z)}{\Phi(r, h) - \Phi(r, 0)} \right)^n dz. \quad (5)$$

Apparently there is no general expression for such an integral for arbitrary n , but it may be calculated for particular values.

4. Generalised Rankine-Hugoniot relation

Let us denote by index 1 the values in TL and by index 2 the values in the disc. Then the mass continuity condition leads to:

$$\rho_{e1} u_1 \zeta_{n,1} = \rho_{e2} u_2 \zeta_{n,2} = j, \quad (6)$$

where, for the sake of brevity, we have redefined (5) as $\zeta_{k,i} = \zeta_k(r_2, h_i)$. The momentum continuity:

$$\rho_{e1} u_1^2 \zeta_{n,1} + p_{e1} \zeta_{(n+1),1} = \rho_{e2} u_2^2 \zeta_{n,2} + p_{e2} \zeta_{(n+1),2} \quad (7)$$

From (6)-(7) we may get the following expression for the mass flux:

$$j^2 = \frac{p_{e2} \zeta_{(n+1),2} - p_{e1} \zeta_{(n+1),1}}{[\rho_{e1} \zeta_{n,1}]^{-1} - [\rho_{e2} \zeta_{n,2}]^{-1}}. \quad (8)$$

The integrated over height energy continuity condition has the following form:

$$h_1 u_1^2 + \zeta_{1,1} w_{e1} = h_2 u_2^2 + \zeta_{1,2} w_{e2}, \quad (9)$$

where w_e – enthalpy at the equator. From (9) taking into account (6)-(8) we may derive the generalization of the Rankine-Hugoniot relation:

$$\frac{h_1 [\rho_{e1} \zeta_{n,1}]^{-2} - h_2 [\rho_{e2} \zeta_{n,2}]^{-2}}{[\rho_{e1} \zeta_{n,1}]^{-1} - [\rho_{e2} \zeta_{n,2}]^{-1}} = \frac{\zeta_{1,2} w_{e2} - \zeta_{1,1} w_{e1}}{p_{e2} \zeta_{(n+1),2} - p_{e1} \zeta_{(n+1),1}}. \quad (10)$$

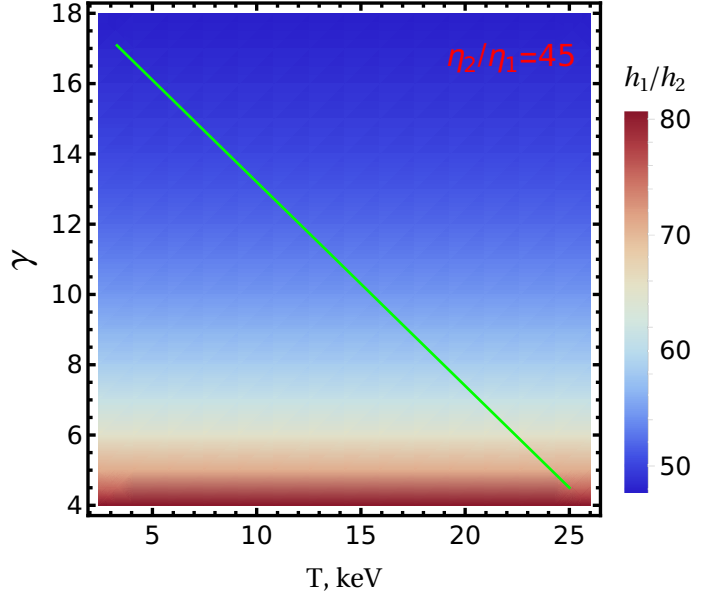


Fig. 2. The dependence of the ratio of the TL height to that of disk h_1/h_2 on the Reynolds number $\gamma_2 = \dot{M}/4\pi h_2 \eta_2$ and temperature in the TL T_1 for the ratio of turbulent viscosities $\eta_2/\eta_1 = 45$. All other calculations were carried out along the diagonal line, which reflects the transition between the high/soft and low/hard states.

If we set homogeneous vertical distribution $\zeta_{k,i} = \zeta_k(r_2, h_i) = 2h_i$ and $h_1 = h_2$ then the usual expression may be gotten:

$$\frac{\rho_{e2}^{-1} + \rho_{e1}^{-1}}{2} = \frac{w_{e2} - w_{e1}}{p_{e2} - p_{e1}}. \quad (11)$$

For a given equation of state and known values of thermodynamic quantities on both sides of the discontinuity, (10) may be considered as an implicit equation relating the heights h_1 , h_2 and the radius r_2 .

5. Rotation

The continuity equation, integrated over the height has the following solution:

$$r \rho_e u \zeta_n = -q, \quad (12)$$

where $q = \dot{M}/2\pi > 0$ is a constant. The equation of force balance in ϕ direction for the TL is the following:

$$\frac{\partial}{\partial r} (r^2 \rho_1 u_1 r \omega_1 - \eta_1 r^3 \omega_1') = 0. \quad (13)$$

Integrated over the height it has the solution $\omega_1 = C_1 r^{-\gamma_1} + C_2 r^{-2}$, where we denoted

$$\gamma_1 = \frac{q}{2h_1 \eta_1} = \frac{\dot{M}}{4\pi h_1 \eta_1}, \quad (14)$$

which is nothing more than the Reynolds number. Before defining the unknown constants, let us discuss the boundary conditions.

In our model, we do not take into account the gradual broadening of the flow after the shock wave, nor its gradual narrowing near the CO. Therefore, neglecting this, we require equality of angular velocities to the disk one at the outer boundary and the CO one at the inner boundary:

$$\omega_1(r_1) = \omega_s, \quad (15)$$

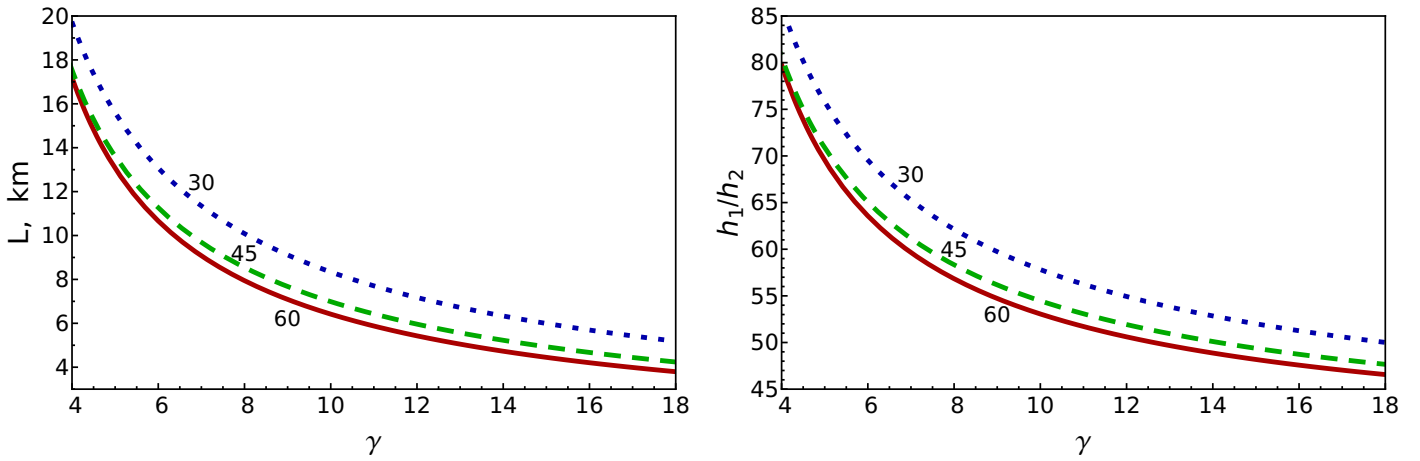


Fig. 3. The dependence of the TL length L (left) and the ratio (right) of the TL height to disk height h_1/h_2 on the Reynolds number, $\gamma_2 = \dot{M}/4\pi h_2 \eta_2$ for different ratios of turbulent viscosities η_2/η_1 : 60 (solid line), 45 (dashed) and 30 (dotted).

$$\omega_1(r_2) = \omega_K(r_2). \quad (16)$$

In addition to the conservation of radial momentum at the discontinuity, there must also be conservation of momentum in the ϕ -direction. Given the viscosity, the law of ϕ -momentum continuity, integrated over height, reads as follows:

$$j\omega_1 - 2h_1\eta_1\omega'_1 = j\omega_2 - 2h_2\eta_2\omega'_2, \quad (17)$$

where j is the mass flux from (6).

Since we suppose that at the outer boundary $r = r_2$ both angular velocities are equal to the Keplerian one (16), then we have the following condition for the angular velocity derivative:

$$\omega'_1(r_2) = \frac{\eta_2}{\eta_1} \frac{h_2}{h_1} \omega'_K(r_2). \quad (18)$$

Thus, for the second-order differential equation (13) we have three boundary conditions (15)(16)(18), i.e. the problem is overdetermined. Using the conditions (15)(16) we may write down the solution:

$$\omega_1 = \frac{1}{r_1^2 r_2^{\gamma_1} - r_1^{\gamma_1} r_2^2} \left(\frac{r_1^2 r_2^2}{r^2} (\omega_K r_2^{\gamma_1} - \omega_s r_1^{\gamma_1}) - \frac{r_1^{\gamma_1} r_2^{\gamma_1}}{r^{\gamma_1}} (\omega_K r_2^2 - \omega_s r_1^2) \right), \quad (19)$$

and (18) may be used to get another implicit equation for h_1 , h_2 and r_2 with given ω_s , $\omega_K(r_2)$ and r_1 . Thus, knowing the CO radius r_1 and height of the accretion disk h_2 , as well as the thermodynamic characteristics of the plasma ρ_e , p_e , w_e on both sides of the discontinuity, the length, and height of the transition layer can be calculated using (10)(18)(19).

6. Setup and results

Since we aim to calculate the geometric characteristics h_1 , r_2 of the TL, in (19) we have switched to the Reynolds number for the disk γ_2 , which is independent of h_1 :

$$\gamma_2 = \gamma_1 \left(\frac{\eta_1}{\eta_2} \right) \left(\frac{h_1}{h_2} \right) = \frac{\dot{M}}{4\pi h_2 \eta_2}. \quad (20)$$

As the CO we considered an NS with a mass of $M = 1.5M_\odot$, a radius of $r_1 = 15$ km and an angular velocity $\omega_s = 10^{-2} \text{ s}^{-1}$. The gravitation potential of the NS is the Newtonian, $\Phi = -GM/(r^2 + z^2)^{1/2}$.

Although in deriving the vertical distributions (3)-(4) it was assumed that the gas is polytropic, the equation of state for the quantities at the equator can, generally speaking, be given arbitrarily; but we considered the same equation of state for vertical and radial dependences. For both TL and accretion disk we took the polytropic index $n = 3$, which corresponds to the photon gas equation of state with $w = 4p/\rho$ and $p = \alpha T^4/3$, where α – radiation density constant, T – temperature.

As a disk height, we took three Schwarzschild radii $h_2 = 3r_S = 13.3$ km. The maximum (at the equator) density and temperature in the disk were taken as $\rho_{e2} = 1.2 \cdot 10^{-5} \text{ g cm}^{-3}$ and $T_{e2} = 0.5$ keV see e.g. ST09.

The density for the TL was chosen to correspond to the observed optical depth relative to Thompson scattering $\tau \simeq 2$ (see e.g. ST09). This value can be achieved by selecting the concentration 10^{17} cm^{-3} which gives $\rho_{e2} = 2 \cdot 10^{-7} \text{ g cm}^{-3}$.

For neutron stars, the TL temperature is around 25 keV in the low/hard state and evolves to approximately 2 keV in the high/soft state (e.g. Seifina & Titarchuk (2010)). In our analysis, there is no way that we can establish a law of temperature change as a function of the mass accretion rate. Therefore, to begin with, we solved (10)(18)(19) for the entire temperature range. As can be seen from Fig. 2 the height of the TL is almost independent of the temperature in it. The same picture is observed for the TL length. However, the solution of (10) with some fixed r_2 alone shows considerable sensitivity to the temperature. The independence of the geometry of the TL on its temperature obtained in our model is achieved only by solving the equations for height and length together. Thus, we can conclude that the geometric characteristics of the TL depend mainly on the accretion rate (Reynolds number γ). Hereafter, these geometric characteristics have been calculated assuming a simple linear relation, $T_1(\gamma_2)$, despite the insignificance of this correction. The relation, $T_1(\gamma_2)$, represented in Fig. 2, reflects the described above transition between the high/soft and low/hard states.

The turbulent viscosity may be estimated in different ways. SS73 proposed its value as $\eta = \alpha \rho c_s l_{\text{turb}}$, where α is a dimensionless constant, c_s is the sound speed, and l_{turb} is a turbulent length scale, which is equal to the height h or, in addition, to the value $(h^{-2} + h_r^{-2})^{-1/2}$, where h_r is the radial pressure scale $h_r = |p/p'|$ (Popham & Sunyaev (2001), PS01 hereafter). Also in radiation-pressure dominated conditions it may be estimated (TLM98) as $\eta = m_p n_{\text{ph}} c l / 3$, where m_p is the proton mass, n_{ph} is the photon number density, c is the speed of light, and l is the

photon mean free path. So the turbulent viscosity may depend on the conditions in the flow as well as its geometry. We avoided further reduction and took several values of the ratio of turbulent viscosities η_2/η_1 to make the resulting TL lengths L to be near the observable ones as well as γ_2 corresponds to α^{-1} parameter from the SS73 model.

We calculated (10)(18)(19) with parameters describes above for three different values of the ratio η_2/η_1 : 30, 45, and 60. When this value is increased, there is no significant change, whereas, at values quite below 30, the length of TL becomes absurdly large.

As can be seen from Fig. 3, the TL length decreases with increasing γ_2 . At extremely low accretion rates, the length of the TL considerably exceeds the radius of the CO, and as it increases, it can drop to tenths of it. The motion of a gas element is a superposition of rotation with an angular velocity ω and falling on the CO with the velocity u , i.e. it is a spiral motion. A smaller radial gas flow (i.e. smaller \dot{M} and γ_2) increases the distance between the coils of such a spiral, thereby making it larger. Therefore, with a fixed viscosity responsible for decreasing the angular momentum, increasing the mass accretion rate leads to decreasing the TL length.

The behavior of the TL height h_1 is similar – it is about 80 times the height of the disk at a low accretion rate and drops to about 45 when the accretion rate increases (see Fig. 3). Thus, the height of the TL of an NS can be up to a thousand kilometers in the low/hard state and half that in the high/soft state. In the frame of our model, this result is quite explainable. The fact is that an increase in the mass accretion rate at a fixed density ρ_2 implies an increase in radial velocity. In this way, more matter flows through a certain area per unit of time, making it smaller.

7. Conclusion

We have solved the problem of the transition layer geometry near a central object (CO). It was supposed to be weakly magnetized, therefore we study only the hydrodynamical properties of such configurations. We have derived the generalized Rankine-Hugoniot relation taking into account different the heights of the accretion disk and TL and heterogeneous distributions along them. Then we solved the equations of continuity and force balance in ϕ direction and have shown that the last one ought to have three boundary conditions. In order to satisfy them, a TL must have certain geometric characteristics.

As a CO we considered NS, setting the gas parameters on both sides of the shock wave according to observations (see ST09). Then the length and height of the transition layer were calculated. We suggest that the turbulent viscosity is constant on each side of the shock, which values have been chosen as such that the Reynolds number γ_2 corresponds to α^{-1} parameter from the SS73 model. As can be seen from Fig. 3, both the TL length and height decrease with increasing γ_2 . Therefore we may conclude that:

1. We clarify the nature of the region where X-ray spectra are formed.

2. When the source evolves to a softer state, the Compton corona region becomes more compact (see Fig. 3 and also ST06, ST09). We should emphasize that the integrated power P_x of the resulting power density spectra rapidly declines toward soft states (TSA07).

3. We should point out that a ratio of the TL height to the disk height h_1/h_2 on the Reynolds number is quite large (see Fig. 3).

4. The calculations were done for a NS, although the same behavior should be expected for other types of COs (a WD and a BH).

5. According to the presented calculations and observed manifestations (ST06, ST09) the TL height h_1 sufficiently exceeds the disk height h_2 . Therefore, as also noted in PS01, one-dimensional constant-height models need to be improved to correctly describe the transition layer.

References

- Abramowicz, M. A. & Fragile, P. C. 2013, *Living Reviews in Relativity*, 16, 1
- Ajay, A., Rajesh, S. R., & Singh, N. K. 2022, arXiv e-prints, arXiv:2210.04997
- Chakrabarti, S. & Titarchuk, L. G. 1995, *ApJ*, 455, 623
- Chakrabarti, S. K. 1989, *ApJ*, 337, L89
- Das, P., Porth, O., & Watts, A. L. 2022, *MNRAS*, 515, 3144
- Farinelli, R. & Titarchuk, L. 2011, *A&A*, 525, A102
- Hōshi, R. 1977, *Progress of Theoretical Physics*, 58, 1191
- Lančová, D., Abarca, D., Kluźniak, W., et al. 2019, *ApJ*, 884, L37
- Liu, B. F. & Qiao, E. 2022, *iScience*, 25, 103544
- Lugovskii, A. Y. & Chechetkin, V. M. 2012, *Astronomy Reports*, 56, 96
- Matsumoto, R., Kato, S., Fukue, J., & Okazaki, A. T. 1984, *PASJ*, 36, 71
- Mishra, B., Kluźniak, W., & Fragile, P. C. 2020, *MNRAS*, 497, 1066
- Popham, R. & Sunyaev, R. 2001, *The Astrophysical Journal*, 547, 355
- Romanova, M. M., Koldoba, A. V., Ustyugova, G. V., et al. 2021, *MNRAS*, 506, 372
- Seifina, E. & Titarchuk, L. 2010, *ApJ*, 722, 586
- Shakura, N. I. & Sunyaev, R. A. 1973, *A&A*, 500, 33
- Shaposhnikov, N. & Titarchuk, L. 2009, *ApJ*, 699, 453
- Strohmayer, T. E., Zhang, W., Swank, J. H., et al. 1996, *ApJ*, 469, L9
- Suková, P., Charzyński, S., & Janiuk, A. 2017, *MNRAS*, 472, 4327
- Sunyaev, R. A. & Titarchuk, L. G. 1980, *A&A*, 86, 121
- Titarchuk, L., Lapidus, I., & Muslimov, A. 1998, *ApJ*, 499, 315
- Titarchuk, L., Shaposhnikov, N., & Arefiev, V. 2007, *ApJ*, 660, 556
- van der Klis, M., Swank, J. H., Zhang, W., et al. 1996, *ApJ*, 469, L1
- Zhang, W., Lapidus, I., White, N. E., & Titarchuk, L. 1996, *ApJ*, 473, L135

MAKE SCIENCE, NOT WAR 